Technical Note

Title: Human adenovirus 40 removal in a side-stream membrane bioreactor

Accepted for publication in Journal of Environmental Engineering on October 26, 2018
Published article DOI: 10.1061/(ASCE)EE.1943-7870.0001525

Alex L. Casabuena, Department of Civil and Environmental Engineering, Michigan State University, East Lansing, MI 48824 USA (casabuen@msu.edu)

Hang Shi, Ph.D., Department of Civil and Environmental Engineering, Michigan State University, East Lansing, MI 48824 USA (shihang2@msu.edu)

Ziqiang Yin, Ph.D. Department of Civil and Environmental Engineering, Michigan State University, East Lansing, MI 48824 USA (yinziqia@msu.edu)

Irene Xagoraraki, Ph.D. Department of Civil and Environmental Engineering, Michigan State University, East Lansing, MI 48824 USA (xagorara@msu.edu)

Volodymyr V. Tarabara*, Ph.D. Department of Civil and Environmental Engineering, Michigan State University, East Lansing, MI 48824 USA (tarabara@msu.edu)

* Corresponding author

Abstract

This preliminary study investigates how the removal of human adenovirus 40 (HAdV 40) in a membrane bioreactor (MBR) depends on the MBR configuration. Results from a side-stream MBR (ssMBR) are compared against data from an immersed MBR (iMBR) and literature data for another iMBR with 0.45 μm pore size hollow fiber membranes used in all three reactors. The central premise of the study is that different fouling mitigation approaches in ssMBR and iMBR lead to differences in membrane fouling and HAdV 40 removals. The hypothesis is tested that the fouling layer acts as an additional separation barrier and is largely responsible for virus removal in MBRs. Higher HAdV 40 rejection observed in ssMBR is attributed to a higher density fouling layer formed in ssMBR under conditions of crossflow shear. The interpretation is supported by the measured differences in the DOC removal and in the $SUVA_{254}$ reduction as well as in the transmembrane pressure response to periodic cleaning in the two MBRs (average decreases in HAdV 40 log removal value of 0.30 and 0.85 in ssMBR and iMBR, respectively). Although the additional energy required to create crossflow in ssMBR does not result in permeate flux enhancement over the iMBR baseline, the denser fouling layer in ssMBR is a more effective barrier for viruses. The trade-off should be considered when weighing the priorities of energy savings and effluent quality.

1. Introduction

Membrane bioreactors (MBRs) play an increasingly important role in water reuse. In comparison with conventional activated sludge reactors, MBRs afford significantly higher pathogen removals (Francy, et al., 2012, Ottoson, et al., 2006). Larger microorganisms such as protozoa and bacteria can be effectively removed by MBRs equipped with membranes with pore sizes of 0.45 µm and smaller (Table 3 in (Yin and Xagoraraki, 2014); Table 2 in (Hai, et al., 2014)). Virus removals in MBRs, however, are usually much lower (Table 4 in (Yin and Xagoraraki, 2014); Table 4 in (Xagoraraki, et al., 2014), Table 3 in (Hai, et al., 2014)) especially for smaller viruses (Figure 7 in (Xagoraraki, et al., 2014); Figure 2 in (Hai, et al., 2014)). Even for membranes with a nominal pore size that is sufficiently small (e.g. 0.04 µm for Zeeweed 500 hollow fibers) to remove larger viruses by size exclusion, complete virus retention is not observed (Yin, et al., 2015). This can be due to defects in the membrane material, other breaches in the treatment system (e.g. leaking glue-lines, connectors and other fittings), or gradual, ageing-induced loosening of the membrane matrix degrading its retention capacity. Since the presence of viruses in the effluent may pose a threat to human health, it is important to understand the mechanisms behind virus removal by MBRs and optimize MBR design to ensure the microbiological quality of the effluent.

The published studies on virus removal in MBRs indicate that the removal is a complex function of the virus type, membrane properties, operational conditions and the state of membrane fouling (Amarasiri, et al., 2017). Indeed, there is growing evidence that membrane fouling plays an important, and in some cases dominant, role in virus

removal in MBRs. Hydraulically irreversible fouling was shown to lead to a sustained improvement of virus removal by membranes (Chaudhry, et al., 2015, Shirasaki, et al., 2008). Yin et al. reported that membrane fouling had a significant impact on HAdV 40 removal by membranes (Yin, et al., 2016, Yin, et al., 2015) showing that the removal correlated with the extent of membrane fouling and that both transmembrane pressure (TMP) relaxation and membrane backwash led to significant (~ 1 log) transient increases in HAdV 40 concentration in treated water (Yin, et al., 2016). Studying removal of adenovirus, norovirus, and F+ coliphage in a full-scale MBR, Chaudhry et al. (Chaudhry, et al., 2015) proposed four mechanisms of virus removal in MBRs and ranked the mechanisms, in the order of decreasing importance, as follows: a) rejection by a cleaned membrane; b) inactivation; (c) rejection by a biofilm (or, to use authors' terminology, "cake layer"); d) virus attachment to mixed liquor solids. To our knowledge, there have been no published studies on virus removal in side-stream MBRs.

The objective of the present work was to investigate how the removal of HAdV 40 depends on the MBR configuration. Specifically, the study explored the premise that different fouling mitigation strategies in iMBR and ssMBR (i.e. aeration and crossflow, respectively) affect virus removal differently with fouling layer properties playing a mediating role. The structure of the fouling layers formed on iMBR and ssMBR membranes can be expected to be different because of the different conditions of the fouling layer formation. Foulants' transport to the membrane surface, packing into the fouling layer, and scouring should all depend on the deposition and removal scenarios that are generally different between the immersed and side-stream MBR configurations. In this study, ssMBR and iMBR were compared side-by-side in terms of TMP buildup,

DOC removal and $SUVA_{254}$ reduction to gain a comparative insight into the fouling processes in these two MBR configurations. The hypothesis tested in the study was that the fouling layer acts as an additional separation barrier and is largely responsible for virus removal in MBRs. HAdV was selected because it is an emerging human health threat with serotypes 40 and 41 being responsible for most cases of adenovirus-associated gastroenteritis in children (Crabtree, et al., 1997, Mena and Gerba, 2009). The choice of HAdV 40 was further motivated by the published data on an incomplete removal of this large (~ 100 nm) virus in MBRs (Simmons, et al., 2011).

2. Materials and Methods

2.1. Membrane bioreactor design and sampling protocol

Activated sludge samples were collected from the East Lansing wastewater treatment plant and conditioned with synthetic wastewater as described previously (Yin, et al., 2016) prior to the start of each MBR. Two membrane configurations were tested (Figure 1; Table S1): immersed (iMBR) and side-stream (ssMBR). The feed tank used in both MBRs was maintained at a constant feed volume of 20 L, continuously aerated at the rate of 0.57 m^3/h. Both the volume of the feed and the aeration rate matched corresponding values used in an earlier study on HAdV 40 removal in an iMBR (Yin, et al., 2016). Each day, 200 mL of synthetic wastewater of the same composition as described earlier (Yin, et al., 2016) was instantaneously added to the MBR feed tank to add nutrients and to compensate for evaporative losses. During MBR operation, mixed liquor suspended solids (MLSS) concentration was ~ 4.5 g/L. Because of the high

hydraulic retention time (100 days, calculated as the volume of the feed divided by the feed flow rate), both ssMBR and iMBR were operated essentially in a batch mode. Daily measurements of MLSS were conducted to ensure that MLSS was constant. Both iMBR and ssMBR were operated in a constant flux regime with a permeate flow rate of 45 mL/min. A custom-written LabView program (Yin, et al., 2016) was used to maintain the constant permeate flow using a proportional-integral derivative algorithm, conduct periodical pressure relaxation by turning the permeate pump on and off, and record data from the flow meter and the pressure sensor. The permeate was drawn using a peristatic digital pump (model 07523-80, Masterflex L/S) and cycled back into the feed tank. Both MBRs had PVDF hollow fiber membranes with the pore size of 0.45 μm and the outer diameter of 1.3 mm. Selection of these larger pore size membranes and the focus on early stages of their fouling targeted the “worst case scenario” in terms of virus removal.

In the iMBR (Figure 1a), four membrane units were assembled by looping the hollow fiber membranes through a short (~ 10 cm) piece of a polytetrafluoroethylene tubing with an inner diameter of ½” and then sealing the tubing using an adhesive (Loctite). Fourteen membrane segments with an effective length of 70 cm were used for each membrane unit yielding 1600 cm^2 of total membrane surface area. The side-stream membrane modules (Figure 1b) were constructed using eight hollow fiber segments with the effective length of 70 cm, packed into long (~ 70 cm) polytetrafluoroethylene tubing (internal diameter of ¼”) and potted (using Loctite adhesive) in two connectors at the ends of the tubing. With four membrane units, the total filtration surface area was 916 cm^2. An additional pump was used to create the crossflow of 1,900 mL/min, which

translated to the crossflow flux of ~ 2.5 cm/s. Because of the lower membrane surface, the permeate flux in ssMBR (~ 29.5 $L \cdot m^{-2} \cdot h^{-1}$) was ~1.75 times higher than in iMBR (~ 16.9 $L \cdot m^{-2} \cdot h^{-1}$).

Each test included two stages: conditioning and fouling. At the conditioning stage, deionized water was filtered through the membranes for 2 h. During the fouling stage the feed was switched to wastewater The fouling stage lasted for 8 days with 30 min cycles of 5 min of programmed TMP relaxation after 25 min of filtration to follow the protocol used in an earlier study on HAdV 40 removal in an iMBR (Yin, et al., 2016). Permeate samples were collected daily using the following multistep procedure timed around a TMP relaxation event: (1) HAdV 40 stock (40 mL) was spiked into the feed tank 6 min before TMP relaxation to allow sufficient time for mixing of spiked viruses by aeration and for sample withdrawal; (2) Feed and permeate samples (50 mL each) were taken 50 s before the same TMP relaxation event; (3) An additional permeate sample (50 mL) was collected ~ 2.5 min after the same TMP relaxation event. At the end of the fouling test the experiment was discontinued, fouled membranes were discarded and new membranes were placed in the tank.

TMP was monitored using a digital pressure sensor (Cole-Parmer 680075-00). A digital flow meter (106-4-C-T4-C10, McMillan) was installed to measure the permeate flow rate. A LabView program was used to periodically relax TMP to reduce membrane fouling as well as record permeate flow and TMP data.

2.2 Dissolved organic carbon (DOC) and UV_{254} absorbance analyses

A portion (40 mL) of each sample was used to measure DOC (model 1010 analyzer; OI Analytical) and UV_{254} absorbance (Spectronic Genesys 2, Milton Roy). The remaining volume was stored at - 80 ^{o}C until used for adenovirus quantification. Normally, DOC is defined as the organic carbon fraction that passes 0.45 μm filter. In this study, however, DOC was operationally defined as the fraction of the organic carbon that passes.0.22 μm pre-filter; this was to avoid the ambiguity caused by the fact that the MBR membranes themselves had the nominal pore size of 0.45 μm. To measure DOC content and UV absorbance of the MBR feed, feed samples were settled for 15 min, the supernatant was then filtered through 0.22 μm membrane and the filtrate was used in the measurements. The settling time was optimized in preliminary tests as the minimal settling duration required for a facile filtration of the supernatant. All TOC and $SUVA_{254}$ values are averages of triplicate samples. Specific UV_{254} absorbance, $SUVA_{254} = UV_{254}/DOC$ (L/(mg·m)) was calculated to assess the aromaticity of dissolved organics (Weishaar, et al., 2003) with higher $SUVA_{254}$ corresponding to more hydrophobic compounds. DOC removal and reduction in $SUVA_{254}$ were calculated as $R_{DOC}\ (\%) = 1 - (DOC)_p/(DOC)_f$ and $R_{SUVA}\ (\%) = 1 - (SUVA)_p/(SUVA)_f$, where indices p and f denote permeate and feed, respectively.

2.3 Quantification of HAdV 40 concentration

Prior to HAdV 40 quantification, virus DNA was extracted from the water samples using QIAamp Viral RNA Mini Kit (Qiagen). HAdV 40 concentration in permeate samples was directly quantified by qPCR using the primers and the probe described previously (Yin, et al., 2016). For feed samples, inhibiting effects of the biomass on DNA extraction and

qPCR could potentially occur. To avoid inhibition, HAdV 40 concentration in stock (40 mL sample) was measured using qPCR prior to spiking the virus into the MBR feed tank (20 L). Log removal value (LRV) of HAdV 40 was calculated as $LRV = -log(C_p/C_f)$, where C_p and C_f have units of genome copies per L. The values of C_f were calculated based on the initial feed concentration of HAdV 40 ($4.27 \cdot 10^7$ copies/mL) adjusted for virus addition due to daily spiking and for virus loss to the permeate.

The average values of the relaxation-induced decrease in LRV were calculated based on the measured LRV decreases during the entire MBR fouling test. The averages for ssMBR and iMBR were then compared using a two tail t-test. The same statistical analysis was applied to examine the statistical significance of relaxation-induced changes in transmembrane pressure. Standard quality control and assurance procedures in calibrating instruments, recording standard curves (e.g. for qPCR) and performing statistical analyses were adapted and used throughout the study.

3. Results and Discussion

3.1. Removal of human adenovirus 40: ssMBR versus iMBR

Figure 2 shows HAdV 40 removal by ssMBR. The LRV was low (0.2 log) early in the filtration process and increased steadily to reach 6.3 logs after 7 days. The increase, together with the observed drops in HAdV 40 LRV after each TMP relaxation event, pointed to the importance of the fouling layer in virus removal. Absolute values of HAdV40 concentration in the feed and the permeate before and after pressure relaxation events are presented in Fig. S1 (see Supplementary Data). Yin et al. (Yin, et

al., 2016) studied HAdV 40 removal by iMBR with the same type of hollow fiber membranes (0.45 μm PVDF), the same aeration rate and filtration/relaxation cycle and the same composition of the synthetic wastewater fed; the removal data reported in that study are provided in Figure 2 for comparison.

The tests in the iMBR performed by Yin et al (Yin, et al., 2016) gave a larger initial removal (~ 2 log) but a slower increase in the LRV of the virus. This behavior can be attributed to a lower shear in the iMBR leading to a faster formation of the fouling layer. In contrast, the crossflow in ssMBR created a high shear near the membrane surface and maintained the membrane relatively fouling-free early in the filtration process; under these conditions, the fouling layer made minimal, if any, contribution, to virus removal, which explains the low LRV values early on during ssMBR operation. In addition, the relaxation events appeared to have a larger impact on virus removal in the iMBR configuration. Indeed, the decrease in LRV for HAdV 40 after TMP relaxation was 0.30 ± 0.16 log on average for ssMBR, which was smaller with statistical significance ($p <$ 0.01) than the 0.85 ± 0.23 average LRV decrease in iMBR (Yin, et al., 2016).

After 7 days of operation, the removal of HAdV 40 in ssMBR was higher than in iMBR even though the permeate flux in ssMBR was higher, which should lead to more virus passage. We attribute the higher LRV observed in the ssMBR to the denser fouling layer formed on membranes in the presence of crossflow. Indeed, the crossflow-induced particle back-transport mechanisms (lift force and shear-induced diffusion) favor particles of larger sizes so that the fouling layer formed in ssMBR should be composed of smaller size fraction of foulants (Altmann and Ripperger, 1997). In contrast, iMBR membranes are susceptible to fouling by particles regardless of particle size. We

hypothesize, that a denser fouling layer develops on ssMBR membranes compared to iMBR membranes. The lower porosity is responsible for the higher rejection of HAdV 40 by the fouling layer, which acts as an additional separation barrier (Choi, et al., 2005).

The LRV data for the two configurations should be compared with caution. First, in the study by Yin et al. (Yin, et al., 2016) the iMBR system was continuously fed with synthetic wastewater while in the present study the ssMBR feed tank was spiked with synthetic wastewater on a daily basis and operated as a near-batch system (Table S1).. To eliminate the potential impact brought about by differences in the feeding regime, a separate set of tests with an iMBR (Figure 1b) was performed using the same hollow fiber membrane and with the same feeding regime as that used in test with the ssMBR; because of the technical constraints, only TMP, DOC and $SUVA_{254}$ (but not HAdV 40) were measured in this iMBR (Table S1).

3.2 Membrane fouling, DOC removal and $SUVA_{254}$ reduction: ssMBR versus iMBR.

Figure 3a shows TMP profiles in the ssMBR and iMBR as functions of time. During each measurement, the TMP values were recorded before and after a TMP relaxation event. For the ssMBR, the decrease in TMP after relaxation was due to the removal of hydraulically reversible fouling layer by crossflow during the TMP relaxation period (i.e. in the absence of permeate flow). The TMP profile recorded for the iMBR was similar to that for the ssMBR indicating that the total hydraulic resistances of the iMBR and ssMBR fouling layers were comparable. The response to TMP relaxation, however, differed: the average relaxation-induced TMP drop in ssMBR (~ 0.9 ± 0.5 psi) was lower

with statistical significance ($p < 0.05$) than in iMBR (~ 1.7 ± 0.5 psi) indicating that a larger hydraulically reversible fraction of the fouling layer on iMBR membranes.

DOC removal (Figure 3b) and $SUVA_{254}$ reduction (Figure 3c) as functions of time were calculated based on a) the values of DOC and $SUVA_{254}$ in the permeate recorded several times during filtration and b) the initial values of DOC and $SUVA_{254}$ in the feed (43.2 mg(DOC)/L and 6.7 L/(g·m)), respectively), recorded once at the start of the filtration test. DOC removal reduction in both MBRs increased with the buildup of the TMP (Figures 3b). Early into the filtration process, unfouled membranes in both MBRs rejected only a small fraction of dissolved organics. As the filtration continued, the fouling layer developed on the membrane surface and functioned as an additional separation barrier. Indeed, DOC removal in ssMBR increased from ~ 11% to ~ 23% (before relaxation) during the 8 days of ssMBR operation. In iMBR, DOC removal was lower (~ 8% to ~ 17% range) than in ssMBR. The results are consistent with the hypothesis that a denser fouling layer forms on ssMBR membranes.

$SUVA_{254}$ is known to positively correlate with the percent aromaticity of DOM (Spencer, et al., 2012, Weishaar, et al., 2003): $SUVA_{254}$ values above 4 L/(mg·m) are taken to indicate that DOM is predominantly hydrophobic (Edzwald and Tobiason, 1999). In the present study, $SUVA_{254}$ in the permeate was in the range from 5.0 to 6.7 L/(mg·m) pointing to a high fraction of aromatic DOC. $SUVA_{254}$ reduction increased with time in both ssMBR and iMBR suggesting a preferential removal of the hydrophobic fraction of DOM by the fouling layer. The lower reduction in $SUVA_{254}$ in ssMBR (observed for all sampling times except at the end of the filtration run) can be explained by the higher rejection of the hydrophilic species by the denser fouling layer in the side-stream system.

Indeed, hydrophilic organic species tend to be smaller because of their lesser propensity to aggregate so that a denser separation layer is required for appreciable rejection of such species. The role of the fouling layer in $SUVA_{254}$ reduction is supported by the fact that the reduction was lower after TMP relaxation events for both iMBR ($\Delta SUVA_{254}$ = 0.15 ± 0.08 L/(mg·m)) and ssMBR ($\Delta SUVA_{254}$ = 0.13 ± 0.08 L/(mg·m)). Another possible explanation is that the microbial decay process is enhanced under the conditions of high hydrodynamic shear in ssMBR; microbial decay can lead to a higher content of aromatic compounds and higher $SUVA_{254}$ in the feed (Dong and Jiang, 2009).

3.3 Role of the fouling layer in virus removal. Implications for MBR design

Similar to the observations reported for iMBR (Yin, et al., 2016), virus removal in ssMBR is shown to decrease in the immediate aftermath of hydraulic cleaning (accomplished by periodic transmembrane pressure relaxation). The finding points to the possibility of permeate recycling the immediate aftermath of membrane cleaning to maximize virus removal in MBRs. The fouling layers formed on iMBR and ssMBR membranes have similar total hydraulic resistance (Figure 3a). The result can be attributed to the formation of thinner but higher specific hydraulic resistance fouling layers in ssMBR due to effects such as shear-induced floc breakup (Zhang, et al., 1997), hydrodynamic selection for smaller foulants (Baker, et al., 1985) and shear-dependent particle packing (Mackley and Sherman, 1992). Together, these crossflow-induced processes negate the cleaning effect of the crossflow shear. The higher specific hydraulic resistance is normally associated with a lower porosity, which is consistent with higher removals of HAdV 40 (Figure 2) and DOC (Figure 3b) observed for the ssMBR. The differences in

the TMP response to periodic cleaning (Figure 3a) and in the higher removal of hydrophilic organics for the ssMBR (Figure 3c) give additional evidence that distinct fouling mitigation strategies (aeration in iMBR vs crossflow in ssMBR) lead to different fouling layer properties. The inference is supported by experimental results indirectly and should be validated by experimental studies of the microstructure of the fouling layer. We note that the same aeration rate was applied in iMBR and ssMBR; however, aeration is also relied upon as the fouling control method in the iMBR, while in the ssMBR membrane fouling is controlled by crossflow. In sum, although the additional energy required to create crossflow in a side-stream system (Chang, et al., 2002, Dijk and Roncken, 1997) does not result in permeate flux enhancement, the crossflow could promote formation of a denser fouling layer, which is a more effective barrier for viruses. The trade-off should be considered when weighing the priorities of energy costs and effluent quality.

4. Conclusions

This preliminary study has explored the effect of membrane fouling on HAdV 40 removal in a side-stream MBR using data from an immersed MBR as a comparative basis. In both ssMBR and iMBR, the virus removal increased with the development of a fouling layer on the membrane surface. Different fouling mitigation strategies – crossflow in ssMBR and aeration in iMBR - were found to affect virus removal differently. The higher HAdV 40 rejection observed in ssMBR was attributed to a lower density fouling layer formed on ssMBR membranes under conditions of crossflow shear. The interpretation is supported by the data on DOC removal and $SUVA_{254}$ reduction in the

two MBRs, and by the differences in the transmembrane pressure response to periodic cleaning. The presented results are preliminary and limited to the specific choice of membrane, virus, MBR feed and operational conditions. To gain a more comprehensive understanding of virus removal in side-stream MBRs, additional studies are warranted.

Acknowledgements

This material is based upon work supported in part by the National Science Foundation grants IIA-1243433 and CBET-1236393.

Supplemental Data

Fig. S1 and Table S1 are available online in the ASCE Library (ascelibrary.org).

References

Altmann, J., and Ripperger, S. (1997). "Particle deposition and layer formation at the crossflow microfiltration." *J. Membr. Sci.*, 124(1), 119-128.

Amarasiri, M., Kitajima, M., Nguyen, T. H., Okabe, S., and Sano, D. (2017). "Bacteriophage removal efficiency as a validation and operational monitoring tool for virus reduction in wastewater reclamation: Review." *Water Res.*, 121, 258-269.

Baker, R. J., Fane, A. G., Fell, C. J. D., and Yoo, B. H. (1985). "Factors affecting flux in crossflow filtration." *Desalination*, 53, 81-93.

Chang, I.-S., Le Clech, P., Jefferson, B., and Judd, S. (2002). "Membrane fouling in membrane bioreactors for wastewater treatment." *J. Environ. Eng.*, 128, 1018-1029.

Chaudhry, R. M., Holloway, R. W., Cath, T. Y., and Nelson, K. L. (2015). "Impact of virus surface characteristics on removal mechanisms within membrane bioreactors." *Water Res.*, 84, 144-152.

Chaudhry, R. M., Nelson, K. L., and Drewes, J. E. (2015). "Mechanisms of pathogenic virus removal in a full-scale membrane bioreactor." *Environ. Sci. Technol.*, 49, 2815-2822.

Choi, H., Zhang, K., Dionysiou, D. D., Oerther, D. B., and Sorial, G. A. (2005). "Influence of cross-flow velocity on membrane performance during filtration of biological suspension." *J. Membr. Sci.*, 248(1-2), 189-199.

Crabtree, K. D., Gerba, C. P., Rose, J. B., and Haas, C. N. (1997). "Waterborne adenovirus: A risk assessment." *Water Sci. Technol.*, 35, 1-6.

Dijk, L., and Roncken, G. C. G. (1997). "Membrane bioreactors for wastewater treatment: The state of the art and new developments." *Water Sci. Technol.*, 35, 35-41.

Dong, B., and Jiang, S. (2009). "Characteristics and behaviors of soluble microbial products in sequencing batch membrane bioreactors at various sludge retention times." *Desalination*, 243, 240-250.

Edzwald, J. K., and Tobiason, J. E. (1999). "Enhanced coagulation: US requirements and a broader view." *Water Sci. Technol.*, 40(9), 63-70.

Francy, D. S., Stelzer, E. A., Bushon, R. N., Brady, A. M. G., Williston, A. G., Riddell, K. R., Borchardt, M. A., Spencer, S. K., and Gellner, T. M. (2012). "Comparative effectiveness of membrane bioreactors, conventional secondary treatment, and chlorine and UV disinfection to remove microorganisms from municipal wastewaters." *Water Res.*, 46, 4164-4178.

Hai, F. I., Riley, T., Shawkat, S., Magram, S. F., and Yamamoto, K. (2014). "Removal of pathogens by membrane bioreactors: A review of the mechanisms, influencing factors and reduction in chemical disinfectant dosing." *Water*, 6, 3603-3630.

Mackley, M. R., and Sherman, N. E. (1992). "Cross-flow cake filtration mechanisms and kinetics." *Chem. Eng. Sci.*, 47, 3067-3084.

Mena, K., and Gerba, C. (2009). "Waterborne adenovirus." *Rev. Environ. Contam. Toxicol.*, 198, 133-167.

Ottoson, J., Hansen, A., Björlenius, B., Norder, H., and Stenström, T. A. (2006). "Removal of viruses, parasitic protozoa and microbial indicators in conventional and membrane processes in a wastewater pilot plant." *Water Res.*, 40(7), 1449-1457.

Shirasaki, N., Matsushita, T., Matsui, Y., and Ohno, K. (2008). "Effects of reversible and irreversible membrane fouling on virus removal by a coagulation-microfiltration system." *J. Water Supply: Res. Technol. - AQUA*, 57, 501-506.

Simmons, F. J., Kuo, D. H. W., and Xagoraraki, I. (2011). "Removal of human enteric viruses by a full-scale membrane bioreactor during municipal wastewater processing." *Water Res.*, 45(9), 2739-2750.

Spencer, R. G. M., Butler, K. D., and Aiken, G. R. (2012). "Dissolved organic carbon and chromophoric dissolved organic matter properties of rivers in the USA." *J. Geophys. Res.*, 117, G03001.

Weishaar, J. L., Aiken, G. R., Bergamaschi, B. A., Fram, M. S., Fujii, R., and Mopper, K. (2003). "Evaluation of specific ultraviolet absorbance as an indicator of the chemical composition and reactivity of dissolved organic carbon." *Environ. Sci. Technol.*, 37(20), 4702-4708.

Xagoraraki, I., Yin, Z., and Svambayev, Z. (2014). "Fate of viruses in water systems." *J. Environ. Eng. ASCE* 140(7), 04014020.

Yin, Z., Tarabara, V. V., and Xagoraraki, I. (2016). "Effect of pressure relaxation and membrane backwash on adenovirus removal in a membrane bioreactor." *Water Res.*, 88, 750-757.

Yin, Z., Tarabara, V. V., and Xagoraraki, I. (2015). "Human adenovirus removal by hollow fiber membranes: Effect of membrane fouling by suspended and dissolved matter." *J. Membr. Sci.*, 482, 120-127.

Yin, Z., and Xagoraraki, I. (2014). "Membrane bioreactors (MBRs) for water reuse in the USA." *The Handbook of Environmental Chemistry*, D. Barceló, and A. G. Kostianoy, eds., Springer Berlin Heidelberg.

Zhang, B., Yamamoto, K., Ohgaki, S., and Kamiko, N. (1997). "Floc size distribution and bacterial activities in membrane separation activated sludge processes for small scale wastewater treatment/reclamation." *Water Sci. Technol.*, 35, 37-44.

394

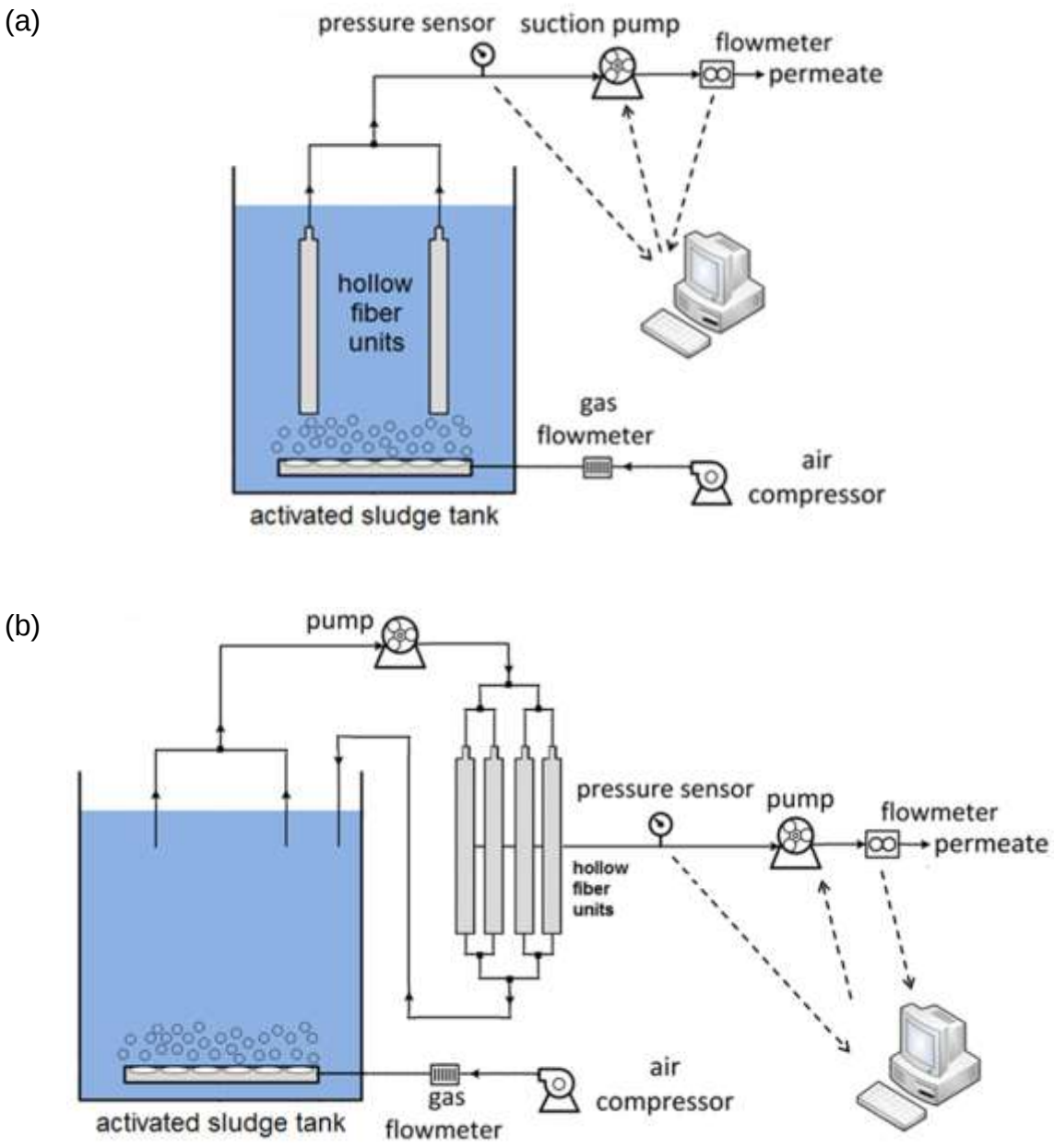

395

396 **Fig. 1.** Schematic illustration of immersed MBR (a) and side-stream MBR (b). In the
397 side-stream MBR, the permeate is cycled back into the feed tank. Details on the
398 operation of each MBR are provided in Table S1.

399

400

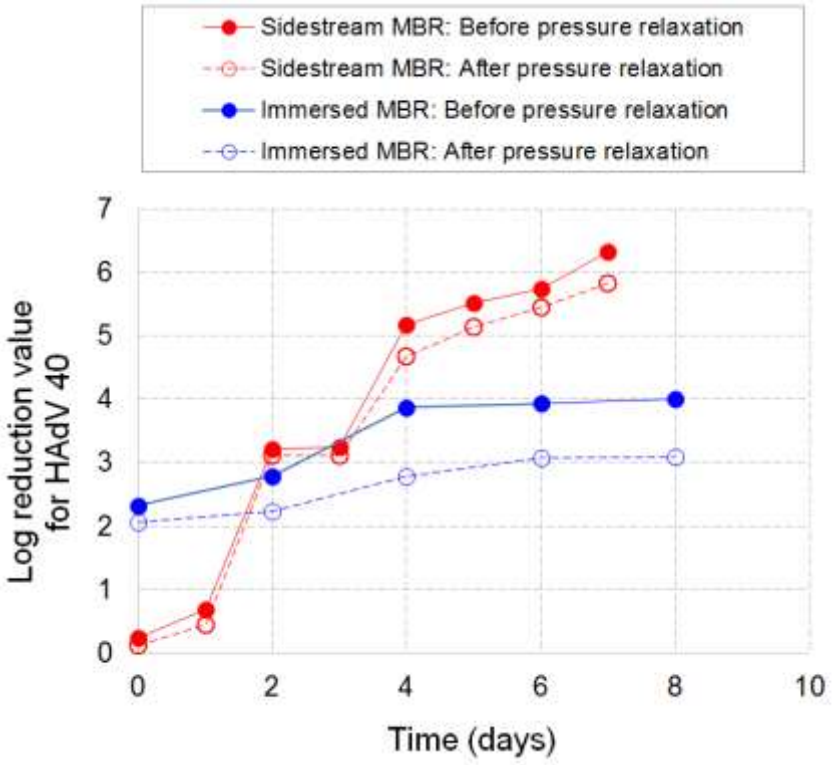

Fig. 2. Effect of pressure relaxation on the removal of HAdV 40 in side-stream and immersed MBRs. Data for the immersed MBR are adapted from Yin et al. (Yin, et al., 2016). Lines are added to guide the eye.

401

402

(a)

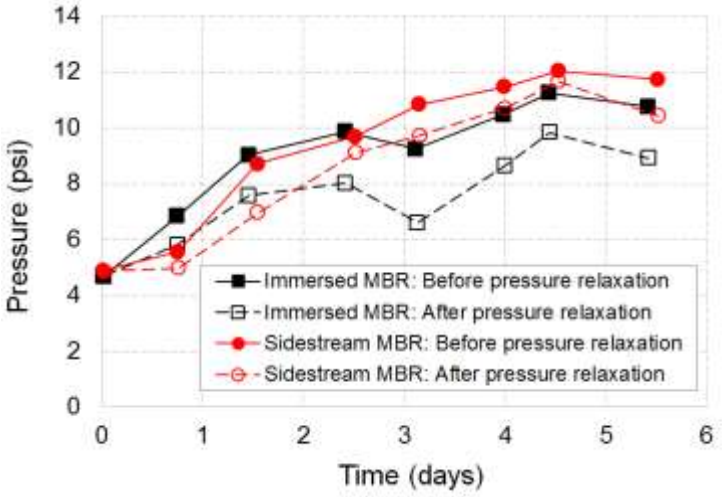

(b)

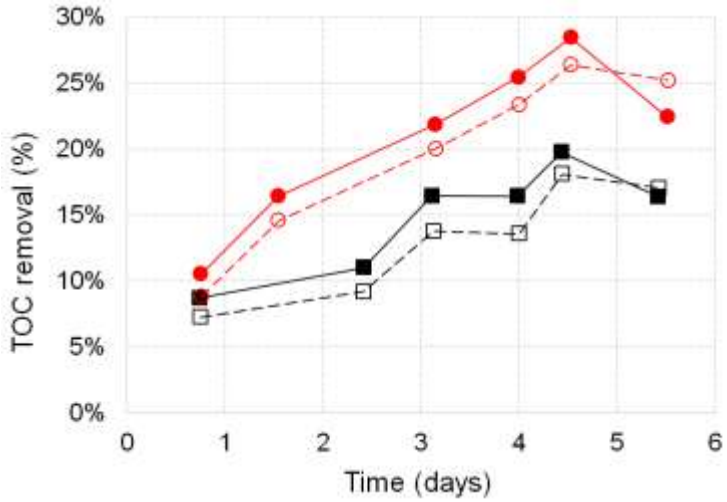

(c)

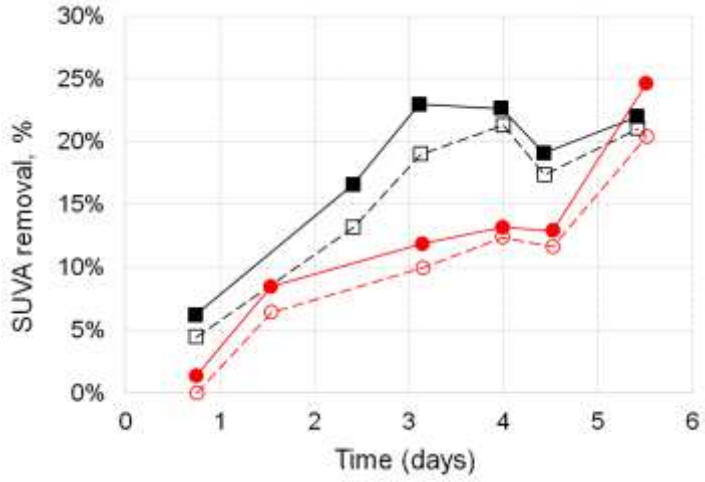

Fig. 3. Effect of pressure relazation on the transmembrane pressure (a), DOC removal (b) and reduction in $SUVA_{254}$ (c) in side-stream and immersed MBRs as functions of filtration time. Values of DOC and $SUVA_{254}$ in the feed are 43.2 mg(DOC)/L and 6.7 L/(g·m), respectively. Lines are added to guide the eye.